GEOGRAPHICAL SEVIRD COVID-19 MODEL WITH TRAVEL RESTRICTIONS

Cristina Ruiz Martin
Nirmal Patel
Gabriel Wainer
Department of Systems and Computer Engineering
Carleton University
1125 Colonel By Drive. K1S 5B6.
Ottawa, ON, CANADA
{cristinaruizmartin, gwainer}@sce.carleton.ca
nirmalpatel3@cmail.carleton.ca

ABSTRACT

Susceptible-Infected-Recovered (SIR) models have been widely used to study the spread of Covid-19. These models have been improved to include other states (e.g., exposed, deceased) as well as geographical level transmission dynamics. In this paper, we present an extension to an existing SEVIRD (Susceptible – Exposed – Vaccinated – Infected – Recovered – Death) model to include the effect of air and maritime travel as well as travel restrictions. We use the model to simulate the spread of Covid-19 through 13 different countries. The case study shown illustrates how the model can be used for rapid prototyping at a geographical level and adapted to include changing policies.

Keywords: Disease Spread, Geographical Modeling, Travel Rules, Cell-DEVS.

1 INTRODUCTION

In late 2019, the COVID-19 disease emerged and spread worldwide in the form of a pandemic. Since then, it is active with at least five variants of concern around the globe (Public Health Ontario, 2022). In the areas where the population density is higher, individuals are more affected by the spread and severity of the virus: a higher number of individuals are infected, resulting in a higher number of deaths. For example, if we compare the Great Toronto Area (GTA) and Ottawa, the GTA has a population density of 4427.8 per km^2 versus 364.9 per km^2 in Ottawa (Statistic Canada, 2021). The cumulative COVID-19 case rate per 100,000 population of the GTA is 9492 compared to 6,199 in Ottawa (Public Health Ontario,2022)

Different countries have imposed different measures to control the spread of the virus, such as curfews, school closures, etc. (Newsroom Ontario, 2021). In some countries, these restrictions also included travel bans; for instance, Canada banned all the direct flights from India during the pandemic outbreak in 2021 (Transport Canada, 2021) or vaccine passports for traveling. Any international traveler has to complete a checklist provided by the Government of Canada to validate their vaccination status (Government of Canada, 2022).

In early 2022, some countries started lifting restrictions; for example, in Switzerland, people could travel without wearing masks, and all other restrictions were also lifted. It is noted that polymerase chain reaction testing returns positivity rates of more than 35% in Switzerland (Stokel-Walker, 2022). New simulation models can help to study the effect of lifting these restrictions.

Since the beginning of the pandemic, several Susceptible-Infected-Recovered (SIR) type models have been developed to study the spread of the virus (Mondal et al. 2020; Kudryashov et al. 2021). Some of these models are based on pre-pandemic research and study the spread of diseases considering geographical aspects. For example, Zhong et al. (2009) presented a mathematical model for epidemiology that considers geographical elements such as the length of the shared border between regions. This model uses cellular automata to simulate the spread of a disease in a geographical environment. Our previous research (Davidson and Wainer 2021) introduced similar geographical models that included other parameters such as asymptomatic individuals, vaccination, etc. We defined a SIRD pandemic model for COVID-19 and used the geography map of Ontario for calibrations and running different simulation scenarios. The model was defined in Cell-DEVS (Wainer 2014) and implemented in Cadmium (Belloli et al. 2019). The model had a restriction: mobility between regions was only possible when there was a land-shared border between regions. This was a reasonable assumption when travel bans and curfews were in place (Newsroom Ontario, 2021). However, when travel restrictions were lifted, we need models to account for air and water travel. This research expands the previous geography-based pandemic models and introduces a more general solution that allows travel rules to include air and road travel. Water travel is modeled as a variation of air travel. Additionally, we improve the modeling of travel restrictions. Previously, travel restrictions were binary in nature; either an individual is allowed to travel, or they are not irrespective of their vaccination status. We have modified the model to consider the vaccination status of individuals on travel restrictions. This improved model allows us to study the effects of lifting travel restrictions considering the number of cases in different countries/regions, the vaccination status, and the public transit routes (road, air, and water) between countries or regions. The model is parameterized so it can be applied at the regional, country, or worldwide level.

To show the model's applicability, we focused on a worldwide level simulation. We compared three different travel restriction strategies: (1) no travel restrictions, that is, an individual can travel to any country (as long as there is a travel route) without any condition; (2) total travel ban from one country to all/some of its neighboring countries to simulate the effect of country-wide lockdown, in which individuals can only interact internally and hence spreading the virus within the country; and (3) a hybrid strategy where some conditions need to be satisfied (e.g., percentage of people fully vaccinated in the country, percentage of people fully recovered from the infection, and percentage of the population currently infected). This hybrid strategy aims to replicate the measures some countries are currently implementing. The results from these three strategies are analyzed and presented.

The rest of the paper is organized as follows. In section 2, we explain the background. Section 3 presents the formal definition of travel behavior and its implementation. Section 4 presents some simulation results and analyses. Finally, section 5 presents the conclusions of our research.

2 BACKGROUND

One of the first SIR-type models was defined in (Kermack and McKendrick, 1927). The authors described a model that classified a given population into three "compartments": Susceptible, Infectious, and Recovered (SIR). Their model specifies how individuals within a population could move from one compartment to another over time based on differential equations. Kermack and McKendrick's work defined the framework and mathematics for the SIR-type models that we continue to follow today. This standard SIR model has evolved over the years to incorporate more advanced disease spread rules and compartments.

Now, most models incorporate a Deceased (D) state (SIRD model) and include death factors and fatality rates (Hethcote 2020). SEIRD models add an Exposed (E) state used to transition from susceptible to infected (Barman et al., 2020). Over time, these models became significantly more advanced, having different, complex compartments such as quarantined (Lin et al., 2020) or diagnosed (Barman et al., 2020), among others.

Another advancement made in SIR-type models was the addition of geographical information. For example, Cardenas et al., (2020) describe a geographical Cell-DEVS SIR model. Their model is based on Zhong et al. (2009) to simulate the spread of epidemics in a geographical-based 2D cell space. Each cell in the model represents a geographical region. At time t, a given cell (i, j) contains a given population Nij and the ratio of individuals in each state. Both Zhong et al. (2009) and Cardenas et al. (2020) use a geographical correlation factor defined by the shared boundaries between two cells. The correlation factor is used to model the interaction between the populations in different regions (i.e., cells).

The equations for the correlation factor between neighborhoods (i.e., cells) are as follows:

$$c_{ij} = c_{ji} = \frac{\frac{z_{ij}}{l_i} + \frac{z_{ji}}{l_j}}{2} \quad (1)$$

Equation (1) describes the weighted correlation factor c_{ij}, which uses the two values, the shared boundary length between cells *i* and *j* (z_{ij}, z_{ji}) in both directions, divided by the total boundary length of cells *i and j* (l_i, l_j). This method states that the correlation for *i*, when moving to *j*, is the same as *j* moving to *i*.

Cardenas et al. (2020) extended the model described in (Zhong et al. 2009) to include parameters that define hospital capacities, lockdowns correction factors, a deceased state, and the ability for recovered individuals to become re-infected. Davidson and Wainer (2021) extend the model with the ability of a cell's population to move from the susceptible state to an exposed state before becoming infected, developing the SEIRD model. When adding the exposed state, the rate at which a cell's population would move from susceptible to exposed remained unchanged. But, when the population moved from susceptible to exposed, a new value was considered, the incubation rate, ε. The exposed state is an important addition to the model as it allows for incubation rate simulations to be added. The model can simulate realistic calculations showing the time it takes for someone to be exposed to when they show symptoms. Fahlman et al. (2021) extended the previous model to account for asymptomatic individuals. The authors defined an asymptomatic rate where a given proportion of the exposed population move to either infectious or asymptomatic. A more recent version of this model (Mereau and Ruiz-Martin, 2021) introduces the impact of vaccination on the spread of COVID-19. The individuals can have different vaccine doses that will affect their susceptibility to the virus

All these models use the above correlation factor, which is not necessarily the most accurate method. Adding transportation networks (Jian et al. 2021) or human movement and mixing models (Kraemer et al. 2019) showing how a population move from one region to another would give more accurate results. We include air and maritime travel and account for traveling restrictions taking into account the vaccination status of the population.

2.1 Cell-DEVS and Cadmium

Cell-DEVS (Wainer, 2014) is a modeling methodology that allows defining cell spaces based on the Discrete Event Systems Specifications (DEVS) (Zeigler et al., 2000). Cell-DEVS describes an n-dimensional cell space where each cell represents a DEVS atomic model. The cell space containing the *n* cells is defined as a DEVS coupled model where each cell is connected to its neighboring cells, as in Figure 1.

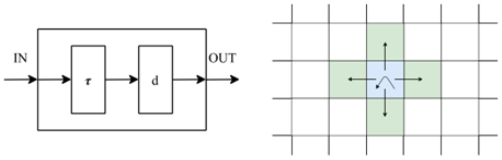

Figure 1. Cell-DEVS model. (left) atomic cell schematics; (right) 2-dimensional Cell-DEVS neighborhood.

When a cell receives an input, the local computing function τ is activated; this will compute the next state for the cell. This discrete-event approach only considers and computes active cells using a continuous-time

base. If there is a change in the cell's state, the change is transmitted after a time delay *d*. In figure 1(b), we can see how a cell (center) will transmit information to the neighboring cells using a von Neumann neighborhood. Cell-DEVS accepts other neighborhoods and irregular topologies as well. Cell-DEVS inherits the modularity and hierarchical modeling ability of DEVS. This allows for models to better interact with other models, tools, datasets, and visualization tools, making it an easy, and efficient method to build complex cellular models.

There are different simulators to execute Cell-DEVS models (Belloli et. al, 2019). In this research, we use the Cadmium tool (Belloli et. al, 2019), which allows users to define model inputs using JavaScript Object Notation (JSON), a data format to store and transmit large amounts of human-readable data. JSON stores data in key-value pairs allowing for the simple representation of neighborhoods, their attributes, and their relationships. Cadmium allows the user to include complex geographical inputs that load into the model at run time resulting in a flexible model that allows for efficient rapid prototyping.

3 SEVIRDS BASE MODEL SPECIFICATION

For this research, we use a SEVIRDS model (Mereau and Ruiz-Martin, 2021) that considers susceptible, exposed, vaccinated, infected, recovered, and deceased individuals. The "S" at the end means that individuals who recovered from the disease can become infected again. The flow of individuals from one state to another is shown in figure 2.

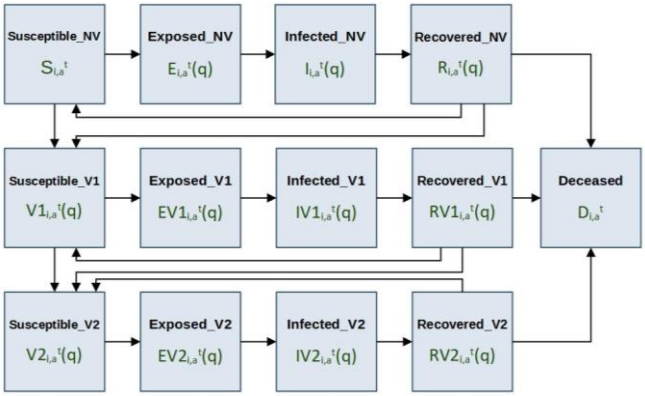

Figure 2: SEVIRDS Model Infection State Diagram.

In the model, we have the three classes of vaccination status (no vaccine, vaccinated with one dose, and vaccinated with two doses). We model the evolution of the vaccination campaigns with a flow of population from less vaccinated states to more vaccinated states. Individuals are only considered for vaccination if they are not in an Exposed, Infected, or Deceased state. In the figure, the bold text indicates the state's name, and the text below each name is the state symbology used in the local computation in the model definition and implementation.

All states that end with the letters "NV" specify the non-vaccinated population. Similarly, all states that end with "V1" specify the population that has received only one dose of vaccine, and all states that end with "V2" specify the population that has received two doses of vaccine**.** Members of the Susceptible_NV and Recovered_NV states are considered eligible for vaccination, and transition to state Suscetible_V1 after vaccination according to the population vaccination rate of dose 1 ($v_{a,d1}$). Members of the Susceptible_V1 and Recovered_V1 states are also considered eligible for vaccination, and transition to state Suscetible_V2 after vaccination according to the population vaccination rate of dose 2 ($v_{a,d2}(q)$). The timing of vaccinations within the states Recovered_NV, Susceptible_V1, and Recovered_V1 are restricted only to the later phases of these states so that a minimum recovered time before vaccination, and a minimum second dose interval is implemented. Members of the vaccinated states have increased protection from infectious exposure specified by immunity rates ($i_{a,d1}$, $i_{a,d2}$), and have incubation rates, recovery rates, and fatality rates that

differ from the non-vaccinated population. When re-susceptibility is enabled, individuals enter the final phase of susceptibility in their vaccination class when they become susceptible again, meaning that in the case of Susceptible_NV and Susceptible_V1, individuals who enter these states as re-susceptible are immediately eligible for vaccination.

The following equation illustrates how the correlation factor is used to calculate the exposed individuals.

$$E_{i,a}^{t+1}(1) = S_{i,a}^{t} \bullet \mathbb{E}_i \tag{2}$$

$$\mathbb{E}_i = \sum_{j \in V}(g_{ij}) \bullet \left[\sum_{b \in A}(a_{j,b}) \bullet \begin{bmatrix} \sum_{q=1}^{T_{i,V1}} \left(\mu V1_b(q) \bullet \lambda_b(q) \bullet IV1_{j,b}^{t}(q) \right) + \\ \sum_{q=1}^{T_{i,V2}} \left(\mu V2_b(q) \bullet \lambda_b(q) \bullet IV2_{j,b}^{t}(q) \right) + \\ \sum_{q=1}^{T_i} \left(\mu_b(q) \bullet \lambda_b(q) \bullet I_{j,b}^{t}(q) \right) \end{bmatrix} \right] \tag{3}$$

$$g_{ij} = c_{ij} \bullet k_{ij} \tag{4}$$

Equation (2) show how the new Exposed_NV (E) population in age group a is equal to the product of the Susceptible_NV (S) population multiply by the neighbor impact factor $\mathbb{E}_i$.

The neighbor impact factor $\mathbb{E}_i$ used to calculate new exposures is shown in Equation 3. The calculation of $\mathbb{E}_i$ sums the amount of infective interaction cell i has with the infected population of all age groups ($a_{j,b}$) in its neighborhood and in all three vaccination status. The infective interactions are factored by the vaccination status, the mobility rates (μ) and the virulence rate (λ). Both virulence and mobility rates are now vaccination dependent. A geo-correction factor (g_{ij}), detailed in equation 4, accounts for the correlation between cells (i.e. if contact between individuals in different cells is possible or not).

As shown in equation 4, the geo-correction factor g_{ij} is the product of the correlation factor c_{ij} (calculated based on the length of the shared border as detailed in equation 1) and an infection correction factor k_{ij}. For each cell, infection thresholds and correlation modifiers are assigned to model each cell's individual set of lockdown policies.

The rest of the paper focuses on the improvements proposed to the geo-correction to account for air and maritime travel and different travel policies.

4 SEVIRDS WITH TRAVEL BEHAVIOR

To better model travel behavior between different regions, we focus on modifications to the geo-correction factor. The modularity in the model definition and implementation allows us to modify how the geo-correction factor is defined without modifying the rest of the equations and their implementation.

Air and maritime travel is modeled updating the correlation factor (c_{ij}) and travel rules are modeled updating the infection correction factor (k_{ij})

4.1 Air and Maritime Travel: A New Correlation Factor

In the original model, the correlation factor was calculated based on the length of the shared land border and the length of the region itself as shown in equation 1. This model of the correlation factor assigns a value of 0 (i.e., not travel is possible) if the two geographical regions are not connected by a land shared border. To have a realistic view of traveling, we need to consider air and maritime travel, which may connect two regions whose land correlation factor is zero. We propose to use the distance between two regions as the parameters to calculate the correlation. Intuitively, the more the distance between two countries, the less correlation factor they will have (i.e., the less likely it is for people to move from one region to the other). For example, traveling from France to Canada is faster and easier than traveling from Australia to Italy. In our model, we will only consider direct flights as the indirect flights will be

automatically accounted for in our direct flights. Although we propose to use the distance between two regions, other criteria may be applied gathering empirical data about the number of people traveling between countries.

The new correlation factor calculation is shown in equation (5). If the two regions share a land border, the correlation factor between the regions is calculated as in the original model based on the shared land border. If the regions do not have shared land border (i.e., $\frac{\frac{z_{ij}}{l_i}+\frac{z_{ji}}{l_j}}{2} = 0$), the correlation factor is calculated considering if there is a flight or maritime route between the regions. In that case, the correlation factor is calculated as a constant (A) divided by the distance between the regions. If there is no route, the correlation factor is zero.

$$c_{ij} = \begin{cases} \frac{\frac{z_{ij}}{l_i}+\frac{z_{ji}}{l_j}}{2} & if\ \frac{\frac{z_{ij}}{l_i}+\frac{z_{ji}}{l_j}}{2} > 0 \\ \frac{A}{dist(i,j)} & if\ \frac{\frac{z_{ij}}{l_i}+\frac{z_{ji}}{l_j}}{2} = 0\ and\ route\ from\ i\ to\ j \\ 0 & if\ \frac{\frac{z_{ij}}{l_i}+\frac{z_{ji}}{l_j}}{2} = 0\ and\ route\ from\ i\ to\ j \end{cases} \quad (5)$$

Practically, the correlation factor is calculated based on the information on a GeoPackage. A GeoPackage is an open, standards-based, platform-independent, portable, self-describing, compact format for transferring geospatial information. There are different software to extract this data from geographical information databases. In our case, we use QGIS (2022) to generate the GeoPackage but other software can be used. Since our model is modular, the correlation factor between two regions can be easily modified by redefining the function. Once the correlation factors have been calculated, the JSON file scenario for the simulation (as explained in section 2.1) can be generated and used to run the simulation.

4.2 Travel Rules: A New Infection Correction Factor

An updated correlation factor is not enough to model realistic traveling. We also need to include travel rules. We updated the model to add rules that enable the population to move from one region to another. This is included in the model modifying how the infection correction factor (k_{ij}) is defined.

Our model handles 3 different scenarios: No Travel Restrictions, Total Travel Restriction, and Partial Travel Restriction.

No Travel Restriction: There are no travel restrictions to enter the specified region. Anyone from another area can enter the region without any conditions. In this case, the infection correction factor (k_{ij}) will be equal to one.

Total Travel Restriction: A region has imposed a complete ban on incoming passengers and closed the borders for individuals from other regions. This strategy will impose a regionwide lockdown, in which individuals are free to move within the region but are not allowed to travel to other regions. In this case, the infection correction factor (k_{ij}) will be equal to zero.

Partial Travel Restriction: A compromise strategy between total and no travel restrictions is partial restrictions. In this strategy, a region can impose different rules for individuals entering the country. Since our model only considers populations in four different states (susceptible, infected, exposed, vaccinated), we can only apply restrictions based on these states. In our case, for the partial restriction strategy, travel is allowed from a region if the following conditions are satisfied:

- 75% of the population from that region is vaccinated, or 75% of the population have recovered
- and less than 10% of the population is infected
- and, if these two conditions are satisfied, only vaccinated individuals can enter the other region.

In this case, infection correction factor (k_{ij}) will be one, but to calculate the neighbor impact factor $\mathbb{E}_i$ (equation 3), when i is not equal to j, we will only consider infected vaccinated individuals.

It is important to remark that in our model, travel restrictions are based on geographical area, and the different regions may have different restriction strategies.

Our model implementation has this travel behavior encapsulated in a function. Therefore, further extensions with other scenarios would just imply adding more flags to the JSON file and a modification on the function that encapsulated this behavior. The rest of the model remains untouched.

5 SIMULATION RESULTS

In this section, we present a simulation scenario to exemplify how to use our model to study and compare different travel policies. The model implementation is available at https://github.com/SimulationEverywhere-Models/Geography-Based-SEIRDS-Vaccinated-Travel-Restriction

We simulate the spread of disease around 13 countries when different travel policies are in place. We used QGIS (2022) to get the GeoPackage and geojson files for generating the scenario and visualizing the results. The countries used along with their population are listed in table 1.

Table 1. Countries used for the simulation scenario.

Country Id	Name	Population		Country Id	Name	Population
1	Australia	25 928 876		8	India	1 399 018 324
2	Canada	38 222 087		9	Japan	125 874 548
3	Germany	83 953870		10	Qatar	2 953 172
4	Denmark	5 822 172		11	Russia	145 903 457
5	Spain	46 739 249		12	USA	333 726 738
6	Ethiopia	119 093 189		13	South Africa	60 349 065
7	France	65 492 887				

To calculate the correlation factor (c_{ij}), on top of the data from the GeoPackage, we provide a CSV file with the relationships for direct route connections (i.e., if it is possible to travel from one country to another by a flight or a maritime route in one day). For instance, the adjacency CSV file will have an entry 2,12 as it is possible to travel from Canada to the USA in one day. The file will also have an entry 12,2 as we can travel from the USA to Canada in a day. If there is no entry from one country to another, it may still be possible to travel; it is just that the passenger will have to go to another country first, and then they can go to the destination. The limitation of this approach is that the travel will take as many days as there are hops in between.

The rest of the section explains the simulation results for this scenario and three different travel strategies.

5.1 No Travel Restriction

We first simulate a strategy with no travel restrictions. In this case, we can expect a steep rise in infections initially while the population is getting vaccinated worldwide. We can also expect that the disease is spread through all the countries. We study two different cases; in the first one, the population cannot be re-infected, and in the second, they can.

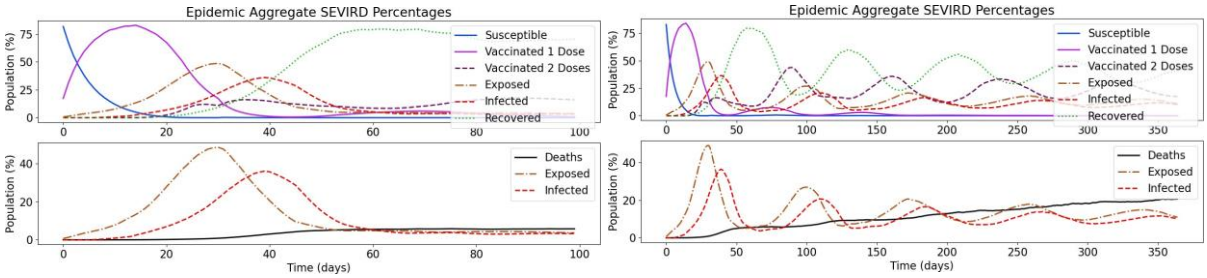

(a) (b)

Figure. 4. Aggregate SEVIRD with vaccination enabled and no travel restriction. (a) no re-susceptibility; (b) re-susceptible.

In figure 4 (a), we present a simulation case study where the population cannot get re-infected. In this case, there is a steep rise in exposure and infections in a very few days while immunity due to the vaccine is developed. After people recover from the disease or after the population grows immunity due to the vaccine, the number of exposed and infected cases drops. This figure shows the aggregate population data for all the countries. We can see how, by allowing travel in the pandemic, there are many infections across the countries. Figure 4 (b) shows the curves when we consider that people may get re-infected with the virus. In this case, we can see different waves with smaller infection peaks as the vaccines take effect. Compared with the previous case, we can also see an increase in deaths.

Although aggregated data is helpful to see the effects of the pandemic worldwide, analyzing how each country is doing is important. To provide those results, we use the Cell-DEVS web viewer (St-Aubin, Hesham, and Wainer, 2018), which generates an animation of the evolution of the pandemic using a geographical map. In figure 5, we can see a snippet of this animation where all the countries have a high infection rate.

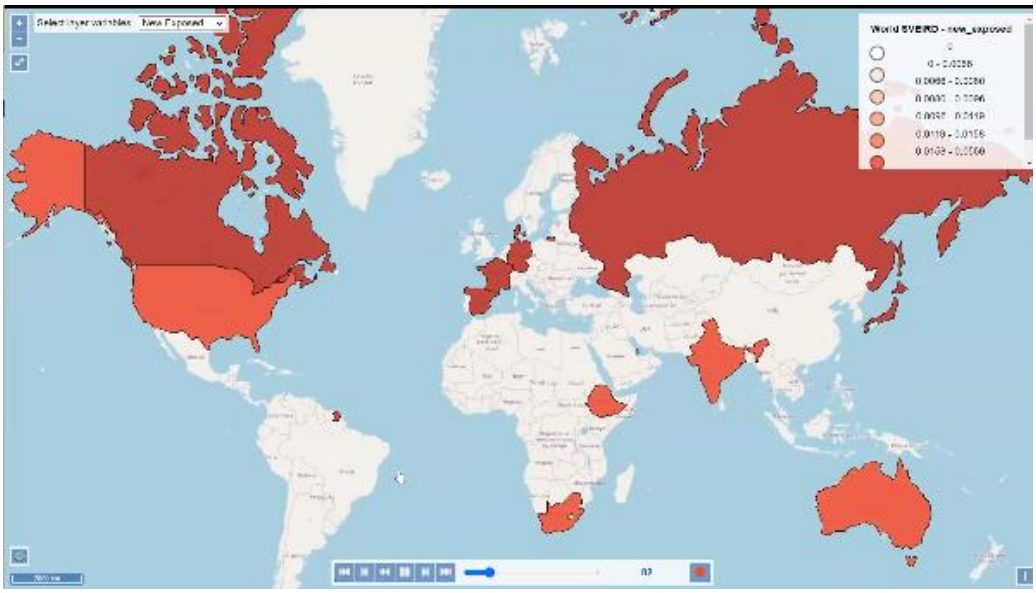

Figure 5. SEVIRD results visualized by country for re-susceptible enabled, vaccination enabled, and no travel restriction.

Figure 6 shows the newly exposed, infected, and recovered population for re-susceptibility disabled and enabled. Focusing on figure 6 (a) (re-susceptibility disabled), we can see a big wave with an infection peak over 4% and a smaller peak (under 1%) over day 60. The exposed and infected population eventually comes down and saturates at 0. In figure 6 (b), when re-susceptible is enabled, we have a first wave similar to the

one in figure 6 (a). However, we have subsequent waves, with lower infection peaks until we get to an steady state when new exposures and infections oscillate between 1 and 2% as vaccines are not 100% effective, and not all the population is vaccinated.

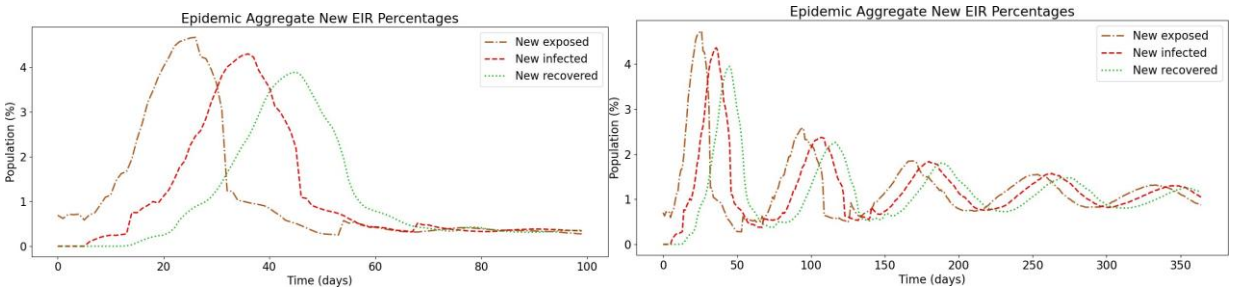

(a) (b)

Figure 6. New Exposed, Infected and Recovered population with no travel restrictions: (a) no re-susceptibility; (b) re-susceptibility.

5.2 Total Travel Restriction

In this case, we simulate a strategy where all travel between countries is banned. We study two different cases; in the first one, the population cannot be re-infected, and in the second, they can. When there is no total travel, we can expect lower values for the infected population compared to the scenario with no travel restrictions.

If we compare figures 4 and 7, only changing travel restrictions from none to total leads to almost half-exposed population peak. Additionally, the peaks occurred later. For example, when we assume no-susceptibility, the infection peak is around day 150 when there are total travel restrictions but around day 35 when there are no restrictions. Whit no travel restrictions, the exposed cases rise to 40% in 20-30 days, while with total travel restriction, total exposed cases rise to 20% after 100 days. This spread in time means it is beneficial for the governments and the medical facilities because they have more time to handle the pandemic better.

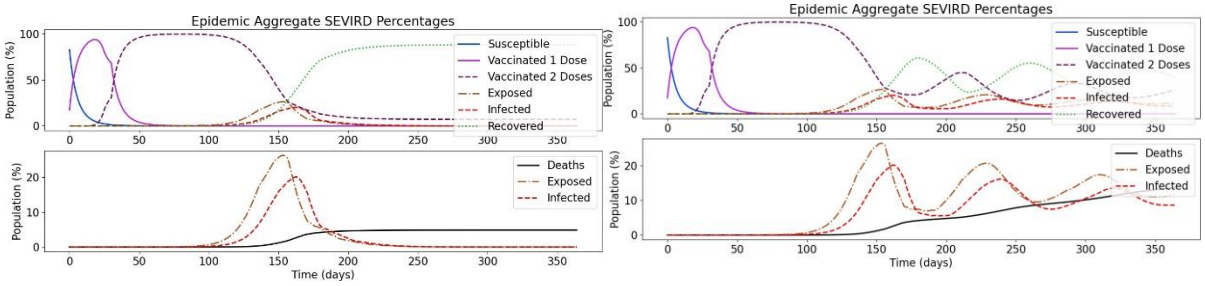

(a) (b)

Figure. 7. Aggregate SEVIRD with vaccination enabled and total travel restriction. (a) no re-susceptibility; (b) re-susceptible.

The reduction and spread in time of the number of infections can also be seen in the new exposed and newly infected population (figure 8). It peeks up around 2.5%, whereas it was more than 4% new cases with no travel restriction. As we can see in the figures, with travel restrictions, the peak occurs later (around day 150), whereas it peaks around day 40 with no travel restrictions.

It is also worth analyzing how the total travel restriction strategy behaves when re-susceptibility is enabled. Comparing figures 7 (a) and (b), there are more infections and more deaths when people can get the disease

more than once. However, when we compare it against no travel restrictions is less severe (around 10% of deaths vs. 20% of deaths) and more spread over time.

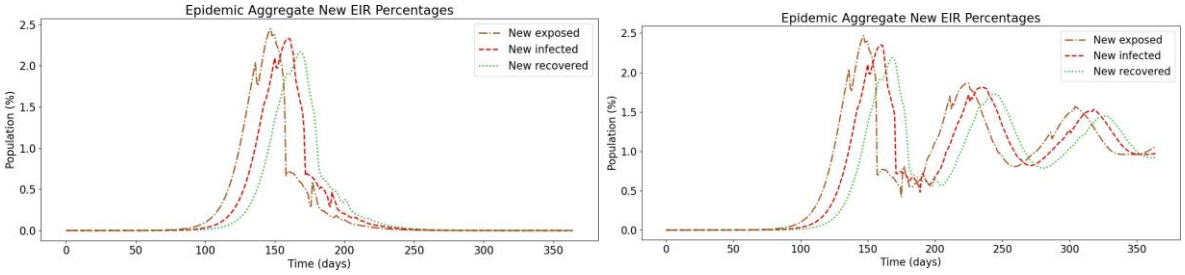

(a) (b)

Figure 8. New Exposed, Infected and Recovered population with total travel restrictions: (a) no re-susceptibility; (b) re-susceptibility.

5.3 Partial Travel Restriction

In this case, we analyze a strategy that falls in between the two strategies we previously discussed. With partial restriction, there are some conditions to travel, such as the vaccination status. As we may intuitively expect, we get results that fall in between the two previous cases.

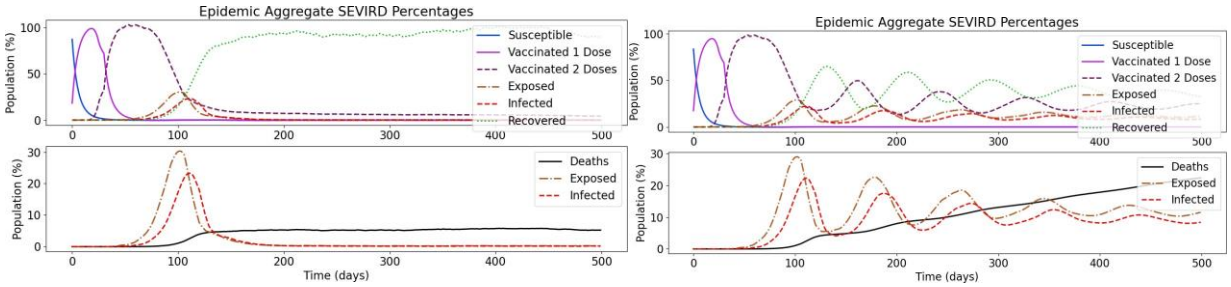

(a) (b)

Figure. 9. Aggregate SEVIRD with vaccination enabled, and partial travel restriction. (a) no re-susceptibility; (b) re-susceptible.

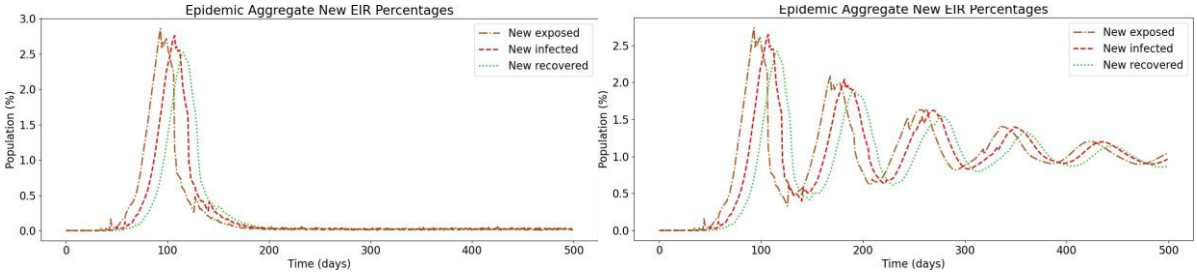

(a) (b)

Figure 10. New Exposed, Infected, and Recovered population with partial travel restrictions: (a) no re-susceptibility; (b) re-susceptibility.

From figure 9 we can say that total exposed cases are lower than no travel restriction (30% compared to 40%), but they are higher than total travel restriction. Also, new exposed cases (figure 10) are higher compared to total travel restriction but again is lower compared to no travel restriction. In terms of number of days it takes to peek the new exposed cases it peeks after around 100 days, where as it has peeked after 150 days with total travel restriction. This is still very late compared to no travel restriction (20 days). This analysis is valid for both re-susceptibility and no re-susceptibility. The difference is that when people can

catch the disease again there are multiple waves and the number of deaths is higher compared to no re-susceptibility.

6 CONCLUSIONS

We presented a model that allows users to create rapid simulation prototypes to simulate the effect of different travel rules and analyze the effect on the spread of the disease. We have addressed the limitation of the previous models where air and maritime travel were not considered. The travel behavior of the model is encapsulated in two coefficients and a travel behavior function. If new geographical information that can affect the spread of the disease becomes available, modelers can easily update the geo-correlation factor and run new simulation scenarios. The model can be extended to cover the asymptotic active cases, new variants, and booster shots for the population. It can also be improved to include dynamic travel restriction policies, where the geo-correlation factor is updated as the simulation evolves based on the availability of new flies or countries changing their travel restrictions policies.

REFERENCES

Barman M., S. Nayak, M. K. Yadav, S. Raha, and N. Mishra, 2020 “Modeling Control, Lockdown & Exit Strategies for COVID-19 Pandemic in India,” *medRxiv*.

Belloli L., D. Vicino, C. Ruiz-Martin, and G.A. Wainer, 2019 “Building Devs Models with the Cadmium Tool”, *Winter Simulation Conference (WSC) 2019*, National Harbor, Maryland, USA

Cárdenas R., K. Henares, C. Ruiz-Martín, and G. Wainer, 2020 “Cell-DEVS Models for the Spread of COVID-19,” *14th International Conference on Cellular Automata for Research and Industry*, Lodz, Poland.

Davidson G., and G. Wainer, 2021 "Studying COVID-19 Spread Using a Geography Based Cellular Model," *Winter Simulation Conference (WSC) 2021*, Phoenix, Arizona, USA.

Fahlman A., C. Ruiz-Martin, G. Wainer, P. Dobias, and M. Rempel, 2021 "Extended Compartmental Model of Covid-19: A Cell-DEVS Definition," *2021 IEEE/ACM 25th International Symposium on Distributed Simulation and Real Time Applications (DS-RT)*, Virtual Event

Geopandas, 2013 https://geopandas.org/en/stable/ Accessed March 28th 2022

Government of Canada, 2022 “COVID-19: Travel, testing, and borders”, online: https://travel.gc.ca/travel-covid Accessed March 28th 2022

Hethcote H.W.,, 2000 “Mathematics of infectious diseases,” *SIAM Rev.*, vol. 42, no. 4, pp. 599–653.

Jian, L., T. Xiang, and L. He. 2021 “Modeling Epidemic Spread in Transportation Networks: A Teview.” *Journal of Traffic and Transportation Engineering*. vol. 8, no 2, p. 139-152.

Kermack W. O. and A. G. McKendrick, 1927. “A Contribution to the Mathematical Theory of Epidemics” *Proc. R. Soc. Lond.*, no. A 115, pp. 700–721

Kraemer, M.U.G., Golding, N., Bisanzio, D. et al. 2019 “Utilizing General Human Movement Models to Predict the Spread of Emerging Infectious Diseases in Resource-Poor Settings”. *Science Reports* vol. 9, no.1 pp. 1-11

Kudryashov N., M. Chmykhov and M. Vigdorowitsch, 2021. “Analytical Features of the SIR Model and their Applications to COVID-19”, *Applied Mathematical Modelling*, vol. *90*, pp. 466–473.

Lin B.C., Y.J. Chen, Y.C. Hung, C.S. Chen, H.C. Wang, and J.L. Chern. 2020 “The Data Forecast in COVID-19 Model with Applications to US, South Korea, Brazil, India, Russia and Italy,” *arXiv*, pp. 1–15.

Mereau E. and C. Ruiz-Martin, 2021, SEVIRDS Model, https://github.com/SimulationEverywhere-Models/Geography-Based-SEIRDS-Vaccinated Accessed March 28th 2022

Mondal A., I. Cooper, and C. Antonopoulos, "A SIR Model Assumption for the Spread of COVID-19 in Different Communities", *Chaos, Solitons & Fractals*, vol. *139*, pp. 110057

Newsroom Ontario, 2021 "Ontario Strengthens Enforcement of Stay-at-Home Order", online: https://news.ontario.ca/en/release/61192/ontario-strengthens-enforcement-of-stay-at-home-order Accessed March 28th 2022

Public Health Ontario. 2022 "Epidemiologic summary: COVID-19 in Ontario – January 15, 2020 to March 27, 2022". https://www.publichealthontario.ca/-/media/documents/ncov/epi/covid-19-daily-epi-summary-report.pdf?la=en Accessed March 28th 2022

Public Health Ontario, 2022. "COVID-19 Variants of Concern (VOCs)", online: https://www.publichealthontario.ca/en/diseases-and-conditions/infectious-diseases/respiratory-diseases/novel-coronavirus/variants Accessed March 28th 2022

QGIS 2022 https://qgis.org/en/site/ Accessed March 28th 2022

Schengen News, 2021, "WHO Calls on World Countries to Lift International Travel Bans", https://www.schengenvisainfo.com/news/who-calls-on-world-countries-to-lift-international-travel-bans/ Accessed March 28th 2022

Statistics Canada. 2021 *Census Profile*. 2021 Census. Statistics Canada Catalogue no. 98-316-X2021001. Ottawa (Released February 9, 2022). Online: https://www12.statcan.gc.ca/census-recensement/2021/dp-pd/prof/index.cfm?Lang=E Accessed March 28th 2022

St-Aubin, B., Hesham O., and Wainer, G. 2018. "A Cell-DEVS Visualization and Analysis Platform", *Summer Simulation Conference*, Bordeaux, France.

Stokel-Walker C., 2022. "COVID Restrictions are Lifting — What Scientists Think", Online: https://www.nature.com/articles/d41586-022-00620-7 Accessed March 28th 2022

Transport Canada, Ottawa, 2021 "Canada Announces Extension of Flight Ban from India as it Prepares for the Return of Direct Flights". Online: https://www.canada.ca/en/transport-canada/news/2021/09/canada-announces-extension-of-flight-ban-from-india-as-it-prepares-for-the-return-of-direct-flights.html Accessed March 28th 2022

Wainer, G. A. 2014. "Cellular Modeling with Cell-DEVS: A Discrete-Event Cellular Automata Formalism". *In Proceedings of the 2014 International Conference on Cellular Automata for Research and Industry*, Kraków, Poland.

Zeigler B., H. Praehofer, and T. G. Kim, "Theory of Modeling and Simulation: Integrating Discrete Event and Continuous Complex Dynamic Systems". San Diego, CA: Academic Press, 2000.

Zhong S., Q. Huang, and D. Song, 2009 "Simulation of the Spread of Infectious Diseases in a Geographical Environment", *Sci. China Ser. Earth Sci.*, vol. 52, no. 4, pp. 550–561.

AUTHOR BIOGRAPHIES

CRISTINA RUIZ-MARTIN is Instructor II at the Department of Systems and Computer Engineering at Carleton University. Her email address is cristinaruizmartin@sce.carleton.ca.

NIRMAL PATEL is an M.Eng student at the Department of Systems and Computer Engineering at Carleton University. His email address is NIRMALPATEL3@cmail.carleton.ca

GABRIEL WAINER is a Full Professor at the Department of Systems and Computer Engineering at Carleton University. He is a Fellow of SCS. His email address is gwainer@sce.carleton.ca.